



ISSN 0975-413X  
CODEN (USA): PCHHAX

Der Pharma Chemica, 2017, 9(19):66-72  
(<http://www.derpharmachemica.com/archive.html>)

## Modeling and Analysis of NO<sub>x</sub> and O<sub>3</sub> in a Street Canyon

Merah Aissa<sup>1,2\*</sup>, Nouredine Abdelkader<sup>2</sup>

<sup>1</sup>Centre for Scientific and Technical Research in Physico-Chemical Analyzes, BP 384, Seat ex-Pasna Zone Industrielle, Bou-Ismaïl PO.Box-42004, Tipaza, Algeria

<sup>2</sup>Laboratory of Applied Mechanics LMA, Oran University of Science and Technology, Mohamed Boudiaf, Algeria

### ABSTRACT

This study numerically investigates reactive pollutants (NO, NO<sub>2</sub> and O<sub>3</sub>) flow and dispersion in a 3D street canyon in time and space, by using a CFD (computational fluid dynamics) code (ANSYS-CFX). An area source (sub-domains) for medium emissions of NO<sub>x</sub> was considered in the presence of background O<sub>3</sub> concentration, with an ambient wind perpendicular to the along-canyon direction. Spatial and temporal variation of pollutants within the canyon was calculated to be significant. It was found that NO and NO<sub>2</sub> concentrations were higher at the upwind buildings (at lower levels near the street bottom) than near the downwind buildings, the largest concentrations of O<sub>3</sub> were observed towards the canyons' windward wall as O<sub>3</sub>-rich air is brought into the canyon.

**Keywords:** ANSYS-CFX, NO<sub>x</sub>, O<sub>3</sub>, Reactive pollutants, Street canyon

### INTRODUCTION

Traffic emission is becoming a major source of air pollution in the urban environment with relatively densely packed buildings flanking narrow streets and continuous increase in motor vehicles. Streets are one of the most important urban elements, where population and traffic density are relatively high [1,2] and human exposure to hazardous substances is expected to significantly increase. Due to the very short distances between sources and receptors, only very fast chemical reactions have a significant influence on the measured concentrations within street canyons [3,4]. For this reason, most traffic-related pollutants (e.g., CO and hydrocarbons) can be considered as practically inert species within these distances. This is not the case either for NO<sub>2</sub>; which dissociates extremely fast in the presence of light, or for NO, which also reacts very fast with O<sub>3</sub> [5]. The time scales of these chemical reactions are of the order of 10 of seconds, thus comparable with residence times of the pollutants in a street canyon.

The chemical composition of the atmosphere has been used as important reference information to help policy-makers define effective emission reduction policies. There are literally thousands of chemical compounds, undergoing an even larger number of chemical reactions in the atmosphere. Because of the current limited computing power, the photochemical models are unable to include all the atmospheric chemical species and reactions simultaneously. Therefore, simplified, or the most representative, chemical mechanisms are introduced into photochemical models to provide a computationally viable means of representing what is understood about the chemical dynamics of trace compounds in street canyons. The CFD modeling approach as a way to understand street canyon flow and dispersion has become powerful and comprehensive with recent advances in computing power, numerical method/algorithm [6,7] and turbulence parameterization [8].

### MATERIALS AND METHODS

#### Numerical simulations

##### *Computational domain of street*

The street canyon was chosen for the study, is one-way street with a length of 95 m (and 10 m of width). This street has about 19 building with heights varying between 3 m and 18 m. The computational domain size is 95 m × 16 m × 21 m (Figure 1a). The emission sources considered in this study are sub-domains (volume sources), created along the street in x direction (11 sub-domains or cars), with size of 3.5 m × 2 m × 1.48 m (Figure 1b).

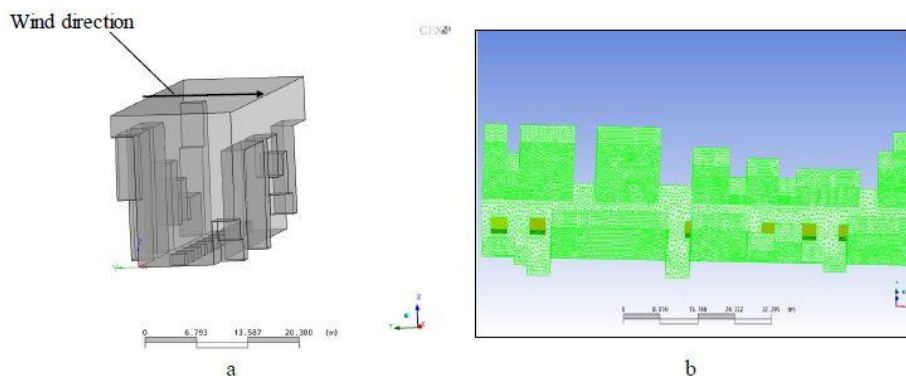


Figure 1: (a) The complete computational domain, (b) Surface mesh elements

### Model description and chemical reactions

The CFD model chosen for this study (ANSYS-CFX) is based on the  $k$ - $\varepsilon$  turbulence model to consider the chemical reaction and the transport of reactive pollutants within a street canyon. The reactive gases considered were NO and NO<sub>2</sub> emitted into the canyon by traffic against a background of ozone. The standard  $k$ - $\varepsilon$  turbulence model governing equations expressed as (Table 1) [9]. The continuity Equation:

$$\frac{\partial U_i}{\partial x_i} = 0 \quad (1)$$

The momentum Equation:

$$\frac{\partial U_i}{\partial t} + U_j \frac{\partial U_i}{\partial x_j} = -\frac{1}{\rho} \frac{\partial \bar{p}}{\partial x_i} + \frac{\partial}{\partial x_j} \left( \nu \frac{\partial U_i}{\partial x_j} - \overline{u'_i u'_j} \right) \quad (2)$$

Where,  $k$  and  $\varepsilon$  transport equations in the standard  $k$ - $\varepsilon$  model:

$$\frac{\partial k}{\partial t} + \vec{V} g \vec{r} a d k = \text{div} \left( \frac{\nu_t}{\sigma_k} g \vec{r} a d k \right) + P - \varepsilon \quad (3)$$

$$\frac{\partial \varepsilon}{\partial t} + \vec{V} g \vec{r} a d \varepsilon = \text{div} \left( \frac{\nu_t}{\sigma_\varepsilon} g \vec{r} a d \varepsilon \right) + \frac{\varepsilon}{k} (C_{\varepsilon_1} P - C_{\varepsilon_2} \varepsilon) \quad (4)$$

Where,  $k$  is the turbulent kinetic energy;  $\varepsilon$  denotes the turbulent dissipation rate.  $P$ : Production of  $k$ ,  $\varepsilon$ : Dissipation of  $k$ . Where,

$$\nu_t = C_\mu \frac{k^2}{\varepsilon}; P = 2\nu_t S_{ij} S_{ij}; \overline{u'_i u'_j} = -2\nu_t S_{ij} + \frac{2}{3} k \delta_{ij}; S_{ij} = \frac{1}{2} \left[ \frac{\partial U_i}{\partial x_j} + \frac{\partial U_j}{\partial x_i} \right]$$

Table 1: The constants for  $k$ - $\varepsilon$  turbulence model

$C_\mu$	$\sigma_k$	$\sigma_\varepsilon$	$C_{\varepsilon_1}$	$C_{\varepsilon_2}$
0.09	1	1.3	1.44	1.92

Pollutant concentration is calculated with the convective-diffusion Equation:

$$\frac{\partial C_i}{\partial t} + U_j \frac{\partial C_i}{\partial x_j} = \frac{\partial}{\partial x_j} \left( K_t \frac{\partial C_i}{\partial x_j} \right) + S_i \quad (5)$$

Where,  $C_i$  denotes the pollutant concentration,  $K_t$  is the eddy diffusivity coefficient and  $S_i$  represents all sources and sinks terms. The chemical reactions considered are:

NO <sub>2</sub> +sunlight ( $\lambda < 420$ nm) $\rightarrow$ NO+(O <sup>3p</sup> )	(r <sub>0</sub> )
(O <sup>3p</sup> )+O <sub>2</sub> +M $\rightarrow$ O <sub>3</sub> +M	(r <sub>1</sub> )
O <sub>3</sub> +NO $\rightarrow$ NO <sub>2</sub> +O <sub>2</sub>	(r <sub>2</sub> )

M represents a molecule (N<sub>2</sub> or O<sub>2</sub> or another third molecule)

The kinetic rate constant (Arrhenius equation) for the reactions r<sub>1</sub> and r<sub>2</sub> is (Table 2):

$$k(T) = A \times T^{\beta} \exp\left(\frac{-E_a}{R \times T}\right) \quad (6)$$

Where,  $A$  is a pre-exponential factor,  $\beta$  is the temperature exponent,  $R$  is the universal gas constant,  $T$  is the temperature, and  $E_a$  is the activation energy.

**Table 2: The parameters for the reactions  $r_1$  and  $r_2$**

Reaction	$A$	$E_a$	$\beta$
$r_1$	$6.10^{-34}$	0.0	-2.3
$r_2$	$2.10^{-12}$	2.782	0.0

The photolysis rate for the reaction  $r_0$  calculated using the expression [10]:

$$J_{NO_2} = 8.14 \times 10^{-3} \times \left[ 0.97694 + 8.14 \times 10^{-4} \times (T - 273.15) + 4.5173 \times 10^{-6} \times (T - 273.15)^2 \right] \quad (7)$$

Where,  $T$  is in K and the unit of  $J_{NO_2}$  is  $s^{-1}$ .

#### Boundaries and initial conditions

The vehicles were assumed to emit NO of  $18.3 \mu g/m^3$ s (90% of  $NO_x$ ), and  $2.03 \mu g/m^3$ s of  $NO_2$  (10% of  $NO_x$ ) for each car [11]. A background ozone concentration of  $70 \mu g/m^3$  (as mass fraction  $f_{O_3} = 5.8 \times 10^{-8}$ ) was then set for the entire domain and the Initial values of mass fraction of  $NO_2$  and NO are  $f_{NO_2} = 2.025 \times 10^{-8}$  ( $24 \mu g/m^3$ ),  $f_{NO} = 1.02 \times 10^{-8}$  ( $12 \mu g/m^3$ ) respectively. At the inflow, the wind velocity assumed as profile (perpendicular to the street) [12] and is given by:

$$U(z) = U_{ref} \left( \frac{z}{z_{ref}} \right)^{\alpha} \quad (8)$$

Where,  $z_{ref}$ ,  $U_{ref}$  are the reference height (10 m) and reference velocity (1.5 m/s), respectively,  $\alpha$  is the power law exponent (0.299), (Figure 2). The pressure and temperature were specified as 1 atm and  $25^\circ C$ , respectively.

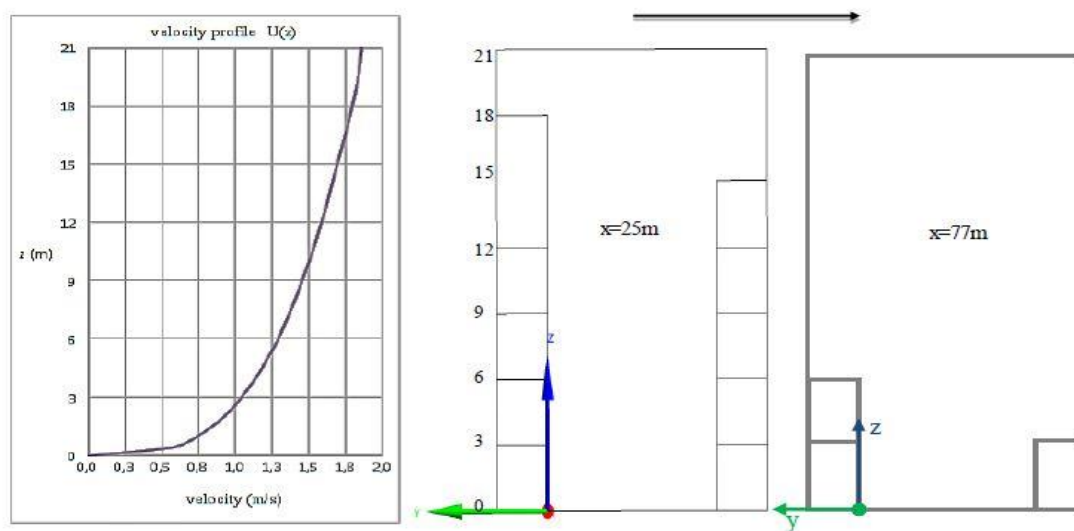


**Figure 2: Velocity profile plot at inflow boundary (left), wind direction perpendicular to the street on x-y plane (at  $x=25$  and  $77$  m positions) (right)**

#### RESULTS AND DISCUSSION

The results presented in Figure 3 show the NO and  $NO_2$  concentration fields and reflects the existence of a vortex in the street canyon for the both positions ( $x=25$  m,  $x=77$  m), the magnitude of pollutant concentrations on the leeward side is larger than the windward side buildings (near the corner of the downwind buildings), due the primary vortex recirculates emitted pollutants therein, and the peak values of NO and  $NO_2$  are  $1.82 \times 10^{-7} \text{ kg/m}^3$ ,  $2.42 \times 10^{-7} \text{ kg/m}^3$  at  $x=77$  m and  $2.4 \times 10^{-7} \text{ kg/m}^3$ ,  $2.5 \times 10^{-7} \text{ kg/m}^3$  at  $x=25$  m, respectively.

On the other hand, there is a formation of  $NO_2$  due to the reactions between  $O_3$  and NO and thus,  $NO_2$  dispersed more significantly than NO [13]. The  $O_3$  concentration is high ( $6.88 \times 10^{-8} \text{ kg/m}^3$ ) near the upper downwind region of the street canyon where ambient ozone intrudes into the canyon [14] and Most exchange takes place near the windward wall where air is entering the canyon from above roof level and pollutants are able to escape [13].

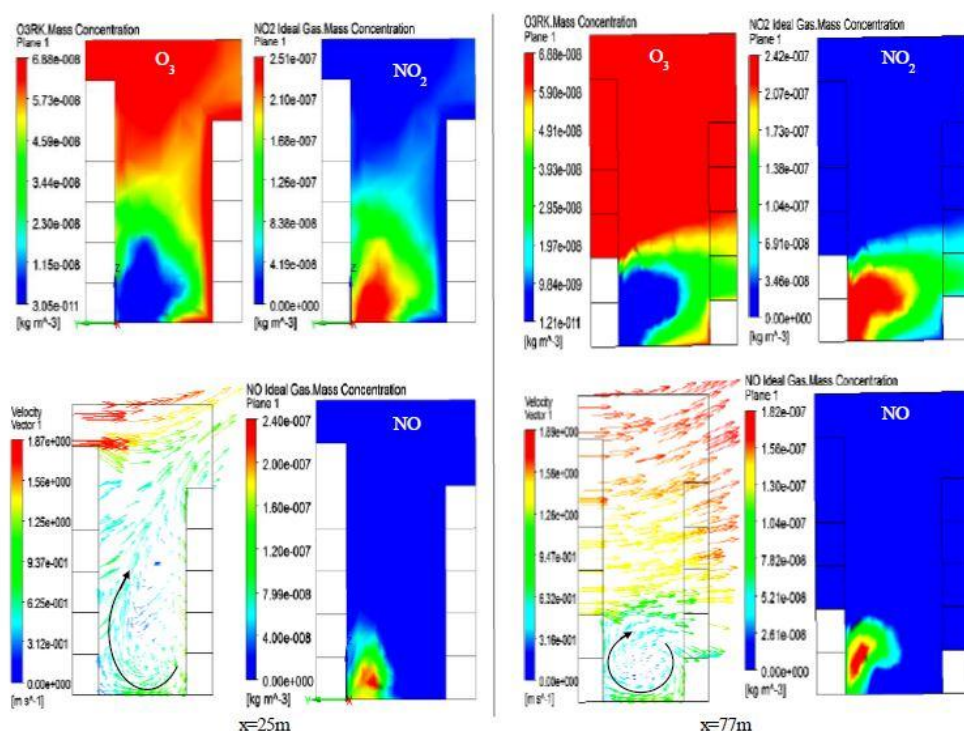


Figure 3: O<sub>3</sub>, NO<sub>2</sub>, NO concentrations and velocity vectors on y-z plane at x=25 m and x=77 m

The Figure 4A presents the correlation between the reactive pollutants for the complete domain (Where the wind direction perpendicular to the street). In Figure 4A (NO<sub>2</sub>/NO graph), it is observed that there is a proportional increase between the concentrations of NO and NO<sub>2</sub>, above the  $1.5 \times 10^{-7} \text{ kg/m}^3$  of NO<sub>2</sub>, this is explain by the increasing of the NO and NO<sub>2</sub> concentrations in leeward wall and in the near the street bottom (in the corner). Under the  $1.5 \times 10^{-7} \text{ kg/m}^3$  of NO<sub>2</sub>, the NO concentration is nearly to zero, because the dispersion of NO is limited than NO<sub>2</sub>. In the Figure 4A (O<sub>3</sub>/NO<sub>2</sub> graph) it can be explained the increasing of the NO<sub>2</sub> concentration with decreasing of O<sub>3</sub> concentration by the consumption of O<sub>3</sub> (by NO) leads to a significant increase of the NO<sub>2</sub> [15].

Last graph (O<sub>3</sub>/NO) in Figure 4A shows that is a disparity in the variation of O<sub>3</sub> concentration with NO (a similar of NO With O<sub>3</sub>) this is explained by the reaction between them near the increasing of NO (in the street corner), and in the regions where the high concentration of O<sub>3</sub>, the NO Concentration is very low (upper downwind region and windward wall). It is very clear that there is a similarity between the graphs of Figure 4A (This study-wind perpendicular to the street) and Figure 4B (Merah et al., wind parallel to the street), this means that the correlation between the pollutants remained almost unchanged, despite a change of wind direction, and thus changed the places of exchange and interaction. Because this correlation reflects the reactions between these pollutants [16,17].

#### Transient simulation (wind perpendicular to the street)

In this part, in the beginning, we have simulated a steady state with presence of a background of ozone, but without the emission of NO<sub>x</sub>. The results from this simulation were used as the initial values file for the transient simulation (90 sec) where the NO<sub>x</sub> emission has been started. The results of the transient case are presented in the Figure 5, which shows the variation of average concentration of O<sub>3</sub>, NO<sub>2</sub> and NO with time for different levels (at x=25 m and 77 m). Firstly, We can observe that the average concentration of NO<sub>2</sub> increases rapidly in the early time in the lower layers and then remains almost constant after 40 sec, and that the concentration decreases as altitude increased (to be almost zero at 12 and 18 m), so for example (at x=25 m) decreases by 25% at 4 m and 60% at 6 m, but for the case of x=77 m where the building heights are 6-3 m, the NO<sub>2</sub> average concentration at the level of 4 m higher than at the level of 2 m, it is due to the escape of pollutants (NO<sub>2</sub>) is significantly above the windward building (3 m) in Figure 3.

Secondly, the reverse is the case for ozone, the average concentration of ozone decreases with a time lag in the lower layers, from the maximum

value  $6.88 \times 10^{-8} \text{ kg/m}^3$  to the lowest values, then remain nearly constant the end of time (after 60 sec). This is associated with NO emission and its dispersion, especially at the lower levels. Therefore, we have noted that ozone decreased by 78% at 2 m, 66% at 4 m and by 36% at 6 m, But at higher levels remained generally steady at the maximum value. Also for x=77 m note that O<sub>3</sub> average concentration at level of 2 m is higher than at level of 4 m, due to the same cause as NO<sub>2</sub> (noted above).

Finally, the average concentration of NO increases with time in the lower layers 2-4 m near the ground, due to the continued emitted from the source, and it takes time to transport to the high levels. for example, for x=25 m, reached  $1.45 \times 10^{-7} \text{ kg/m}^3$  at 2 m in 90 sec, also observed that the concentrations of NO for x=25 m is generally greater than for x=77 m, this due to its consumption by ozone is significantly there, It also becomes non-existent in the upper levels.

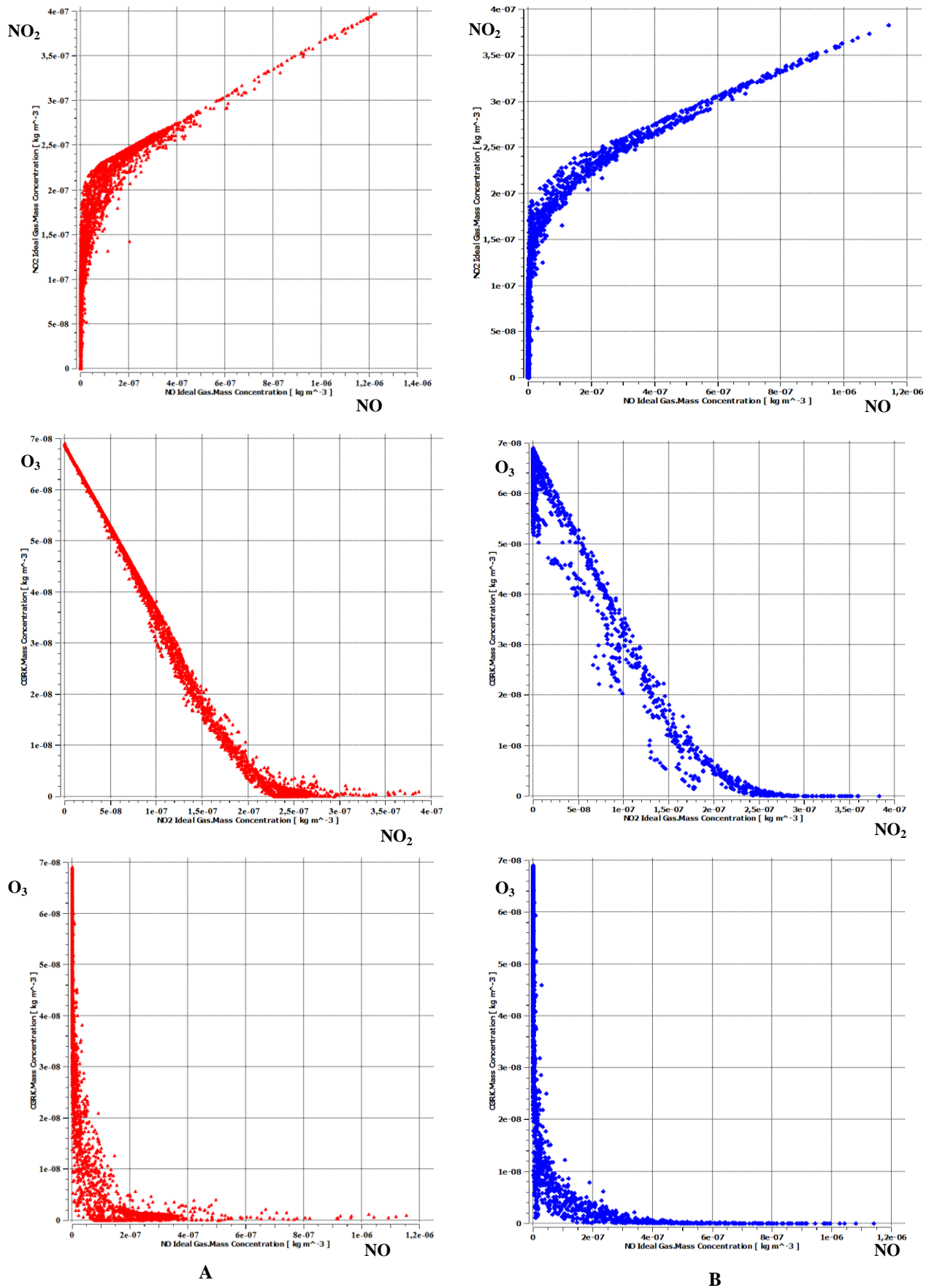


Figure 4: Domain average concentrations correlation: NO<sub>2</sub> with NO, O<sub>3</sub> with NO<sub>2</sub>, and O<sub>3</sub> with NO A-This study (wind perpendicular to the street), B-Merah et al., 2016 (wind parallel to the street)



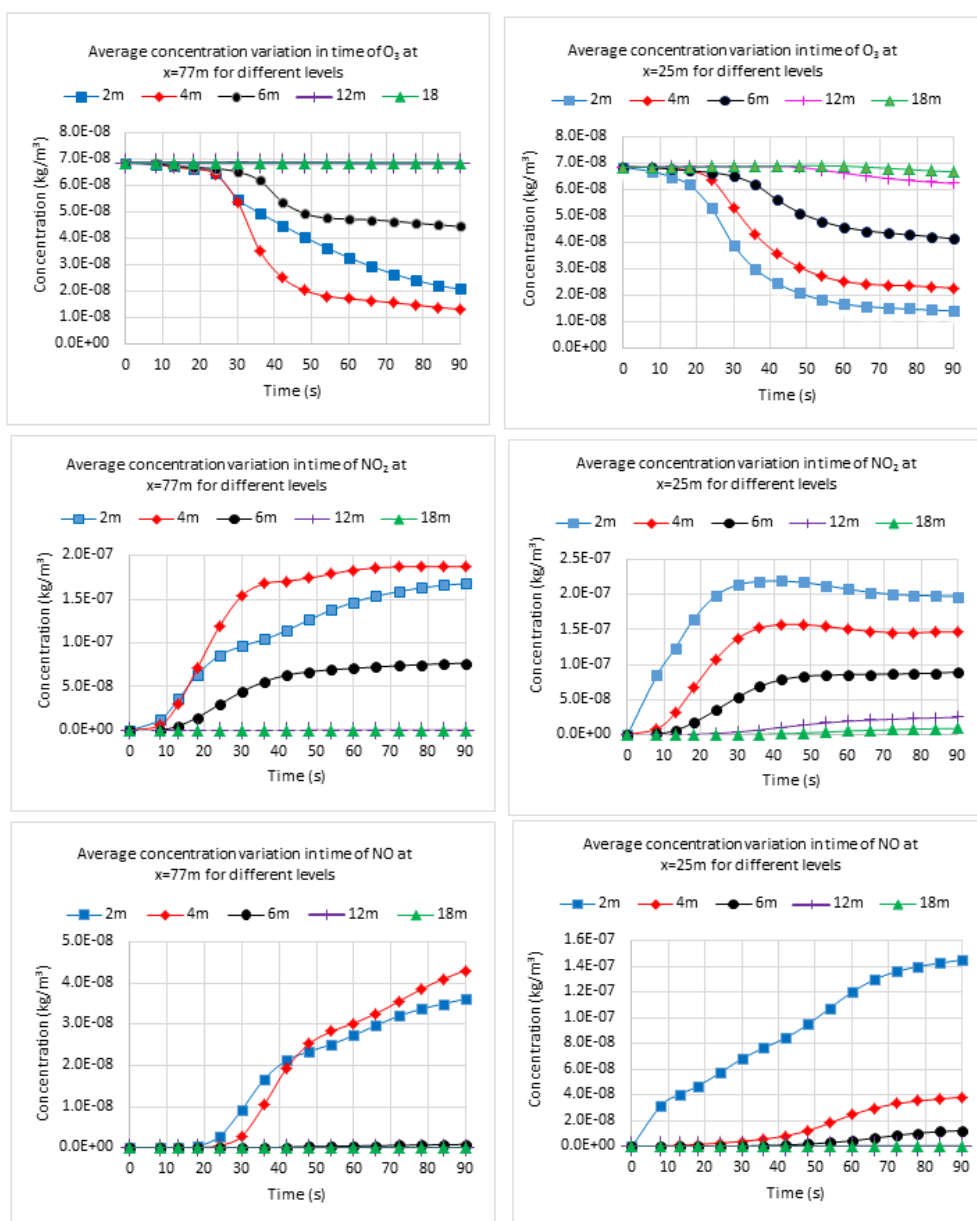


Figure 5: Average concentration variation in time of  $\text{O}_3$ ,  $\text{NO}_2$  and  $\text{NO}$  for different levels at: (left)  $x=77\text{m}$ , (right)  $x=25\text{m}$

### CONCLUSION

The results indicated that the wind perpendicular to the street leads to accumulation of pollutants inside the street canyon with a different degree depending on buildings height, as the height of buildings increases, the pollution level increases, that is, the concentration ( $\text{NO}$ ,  $\text{NO}_2$ ) is higher near the downwind building than near the upwind building, due the vortex recirculates emitted pollutants therein. The highest within-canyon concentrations of  $\text{O}_3$  were observed near the upper downwind region of the street canyon where ambient ozone intrudes into the canyon. It is interesting to observe that under the increasing buildings height the amount of intrusion of ambient ozone into the canyon has been increased. It is indicated that increment of building height encourages the accumulation of ozone. On the other hand when compared this study with (Merah et al.,) it found that the correlation between the pollutants remained almost unchanged, despite a change of wind direction, and thus changed the places of exchange and interaction. Because this correlation reflects the reactions between these pollutants.

### ACKNOWLEDGEMENT

The authors are indebted to Laboratory of applied mechanics LMA (USTO-MB University) for all support and the facilities provided.

### REFERENCES

- [1] P. Kastner-Klein, P.J. Plate, *Atmos. Environ.*, **1999**, 33, 3937-3979.
- [2] R.N. Meroney, M. Pavageau, *J. Wind. Eng. Ind. Aerodyn.*, **1996**, 62, 37-56.
- [3] J. Baker, L. Walker Helen, X. Cai, *Atmos. Environ.*, **2004**, 38, 6883-6892.
- [4] M.W. Rotach, *Atmos. Environ.*, **1995**, 29, 1473-1486.
- [5] P. Finn, B. Ruwim, H. Ole, V. Elisabetta, *Sci. Total. Environ.*, **1996**, 189/190, 409-415.

- [6] T.R. Oke, *Energ. Bldg.*, **1988**, 11, 103-131.
- [7] W.C. Cheng, L. Chun-Ho, D.Y.C. Leung, *Atmos. Environ.*, **2009**, 43, 3682-3690.
- [8] B. Jong-Jin, K. Jae-Jin, *J. Appl. Meteo.*, **1999**, 38(11), 1576-1589.
- [9] J.F. Sini, S. Anquetin, G. Mestayer, *Atmos. Environ.*, **1996**, 30, 2659-2677.
- [10] J.J. Baik, J.J. Kim, *Atmos. Environ.*, **2002**, 36, 527-536.
- [11] A. Merah, A. Noureddine, M. Abidat, *Der. Pharma. Chemica.*, **2016**, 8, 418-424.
- [12] T. Yoshihide, M. Akashi, Y. Ryuichiro, K. Hiroto, N. Tsuyoshi, Y. Masaru, S.T Shirasawa, *J. Wind. Eng. Ind. Aerod.*, **2008**, 96, 1749-1761.
- [13] V.B. Bright, W.J. Bloss, X. Cai, *Atmos. Environ.*, **2013**, 68, 127-142.
- [14] J.J. Baik, Y.S. Kang, J.J. Kim, *Atmos. Environ.*, **2007**, 41, 934-949.
- [15] A.G. Triantafyllou, S. Zoras, V. Evagelopoulos, S. Garas, C. Diamantopoulos, *Global. NEST. J.* **2008**, 10, 161-168.
- [16] M. Yucong, L. Shuhua, Z. Yijia, W. Shu, L. Yuan, *J. Adven. Meteo.*, **2014**, 458671.
- [17] G.T. Johnson, L.J. Hunter, *Atmos. Environ.*, **1999**, 33, 3991-3999.